

Luminescent Iridium(III) Pyridinium-Derived N-Heterocyclic Carbene Complexes as Versatile Photoredox Catalysts

Tsz Lung Lam,^{*,†} Jing Lai,[†] Rajasekar Reddy Annapureddy,^{‡,§} Mingyong Xue,[†] Chen Yang,[‡] Yunzhi Guan,[†] Pingjian Zhou,[†] and Sharon Lai-Fung Chan^{*,§,||}[†]Department of Applied Biology and Chemical Technology, The Hong Kong Polytechnic University, Hung Hom, Hong Kong, P. R. China[‡]State Key Laboratory of Synthetic Chemistry, Institute of Molecular Functional Materials and Department of Chemistry, The University of Hong Kong (HKU), Pokfulam Road, Hong Kong, P. R. China

Supporting Information

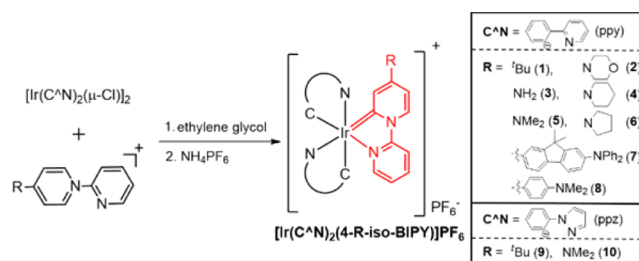
ABSTRACT: The development of novel luminescent iridium(III) complexes with highly tunable emission energy and versatile applications is of particular importance. In this Communication, a series of luminescent iridium(III) complexes supported by chromophoric pyridinium-derived N-heterocyclic carbene (NHC) ligands that display tunable emission from 516 to 682 nm were prepared. These complexes can be used as photocatalysts in photooxidation and photoreduction reactions and could have potential applications in pH sensing.

Pyridinium-derived N-heterocyclic carbene (NHC) ligands (pyridylidene), *N*-(2-pyridyl)-4-*R*-pyridine-2-ylidene (4-*R*-iso-BIPY), first introduced by Bercaw and co-workers as a class of robust ligands for Shilov Chemistry,¹ are deemed to have the combined features of robustness of the metal–NHC bond and rich photophysics of diimine ligands arising from the low-energy π^* orbitals. Nonetheless, the coordination chemistry of 4-*R*-iso-BIPY is largely unexplored.^{1,2} While there are a number of reports on the analogous metal “bipyridinium-like” NHC complexes, most of them focused on structural or catalytic studies,³ except the recent work on iridium(III) *N*-methylbipyridinium complexes by Coe and co-workers.^{3f,g} In this regard, we are attracted to using the 4-*R*-iso-BIPY ligands to design new luminescent cationic Ir^{III}-NHC complexes because the former could be easily prepared and structurally modified, leading to easy access to diverse NHC ligands having tunable low-energy π^* orbitals. More importantly, cationic cyclometalated iridium complexes, particularly those with diimine ligands, are documented to have vast applications in electroluminescent devices,⁴ photoinduced hydrogen production,⁵ chemosensors,⁶ bioimaging,^{6b,7} and photoredox catalysts for organic transformations.⁸ The applied studies of their NHC counterpart, however, have received less attention.^{9–11} Herein we describe novel luminescent cationic cyclometalated iridium(III) complexes supported by the 4-*R*-iso-BIPY ligands and their applications as strong photoreductants and photooxidants in photochemical reactions and for pH sensing.

The 4-*R*-iso-BIPY ligands (L1–L8) were prepared by a one-pot reaction in fair-to-excellent yields (37–98%; Scheme S1). Complexes [Ir(C[^]N)₂(4-*R*-iso-BIPY)]PF₆ [**1**–**10**; C[^]N = 2-phenylpyridine anion (ppy) or 1-phenylpyrazole anion (ppz)]

were synthesized in 19–47% yield by refluxing a mixture of [Ir(C[^]N)₂(μ -Cl)]₂ and L1–L8 in ethylene glycol for 12 h under argon followed by anion metathesis and chromatographic workup (Scheme 1). A downfield ¹³C NMR signal in the range

Scheme 1. Synthesis and Chemical Structures of 1–10



of 174.3–188.1 ppm, characteristic of a metalated NHC carbonic C resonance, was observed for **1**–**10**.^{3g,9,11,12} Diffraction-quality crystals were obtained for **1**, **2**, **5**, and **10** (Figure S1). A facial arrangement for pyridinic/pyrazolic N (i.e., C trans to N) is observed in all of these complexes. The Ir–C_{carbene} distances range from 1.962(3) to 1.976(6) Å (Table S1), which are comparable to literature values with carbene trans to the pyridine ring.^{3f,12b} Interestingly, analysis of **2**, **5**, and **10** suggests extensive delocalization of π electrons from the –NR₂ substituents into the pyridylidene ring (Figure 1), which is evidenced from the

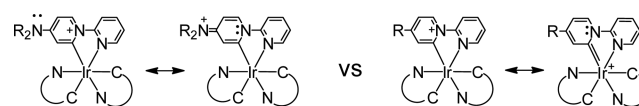


Figure 1. Resonance structures of [Ir(C[^]N)₂(4-*R*-iso-BIPY)]⁺ with and without the –NR₂ substituent.

following: (i) *sp*² hybridization of N atoms in the NMe₂ and NC₄H₈O groups (\angle RNR = 115.2–119.0°); (ii) torsional angle between –NR₂ and the pyridylidene ring close to 0° (1.6–7.9°); (iii) variable-temperature ¹H NMR measurements of **5**, indicating a restricted rotation of the C–NMe₂ bond with $\Delta G^\ddagger_{\text{rot}} = 14.9$ kcal/mol (Figure S2); (iv) ¹³C NMR data of Ir–

Received: April 20, 2017

Published: August 28, 2017

$\epsilon_{\text{carbene}}$ of **2**, **5**, and **10** being less deshielded than that of **1** (188.1 ppm for **1** vs 174.3–178.8 ppm for **2**, **5**, and **10**).

The photophysical data of **1**–**10** are listed in Tables 1 and S3. Figure 2 depicts UV–vis absorption spectra of **1** and **5** in

Table 1. Photophysical Data of 1–10

	Abs $\lambda_{\text{max}}/\text{nm}^a$ ($\epsilon \times 10^3/\text{M}^{-1}\text{cm}^{-1}$)	Em $\lambda_{\text{max}}/\text{nm}^a$ ($\tau/\mu\text{s}; \phi^b$)
1	276 (33.5), 374 (9.0), 403 (sh) (6.0), 494 (0.8)	596 (0.1; 0.06)
2	269 (36.5), 288 (33.4), 332 (33.2), 342 (35.6), 377 (16.8), 460 (2.1)	546 (0.9; 0.33)
3	266 (42.0), 294 (40.4), 310 (37.9), 322 (sh) (32.9), 367 (14.3), 459 (1.6)	537 (1.0; 0.37)
4	276 (36.6), 286 (34.9), 333 (33.0), 343 (37.0), 376 (19.6), 459 (2.2)	533 (1.6; 0.53)
5	261 (37.9), 279 (36.0), 321 (33.6), 331 (37.2), 362 (18.1), 446 (2.4)	522 (2.1; 0.78)
6	274 (38.0), 289 (36.2), 331(34.1), 342 (39.0), 372 (20.1), 452 (2.5)	516 (2.2; 0.81)
7	257 (56.5), 277 (51.3), 311 (39.4), 337 (39.2), 494 (22.4)	682 (1.8; 0.19)
8	257 (46.5), 278 (43.4), 382 (14.0), 411 (16.4), 474 (42.2), 520 (sh) (12.6)	607 (3.0; 0.04)
9	315 (10.0), 385 (5.2), 485 (1.0)	586 (0.2; 0.02)
10	320 (33.4), 330 (35.6), 359 (13.6), 430 (1.9)	516 (2.4; 0.35)

^aMeasured in a degassed CH_2Cl_2 solution at 2×10^{-5} M for **1**–**6** and **8**–**10** and 5×10^{-6} M for **7** at 298 K. ^bPhosphorescence quantum yields were measured using an integrating sphere.

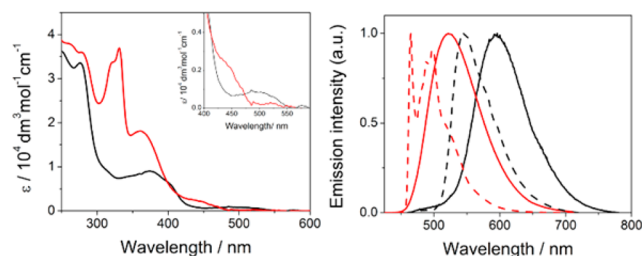


Figure 2. Left: UV–vis absorption spectra of **1** (black line) and **5** (red line) in CH_2Cl_2 at 298 K. Right: Emission spectra of **1** (black line) and **5** (red line) in degassed CH_2Cl_2 at 298 K (solid line) and in alcoholic glass [1:4 (v/v) methanol/ethanol] at 77 K (dashed line).

CH_2Cl_2 . The strong absorption bands for **1** and **5** at $\lambda < 300$ nm [$\epsilon = (33.5\text{--}37.9) \times 10^3 \text{ M}^{-1} \text{ cm}^{-1}$] are assigned as $^1\pi\pi^*$ transitions of ppy and 4-R-iso-BIPY (Figure S3). The additional intense absorption band at $\lambda_{\text{max}} = 331$ nm ($\epsilon = 37.2 \times 10^3 \text{ M}^{-1} \text{ cm}^{-1}$) for **5** is assigned as the $^1\pi\pi^*$ transition of LS. The moderately intense bands at 330–430 nm for **1** are assigned as an admixture of singlet metal-to-ligand charge-transfer ($^1\text{MLCT}$) and ligand-to-ligand charge-transfer ($^1\text{LLCT}$) transitions from $d\pi(\text{Ir}) \rightarrow \pi^*(\text{pyridylidene})$ and $\pi(\text{ppy}) \rightarrow \pi^*(\text{pyridylidene})$, whereas that at 347–413 nm for **5** is assigned as $^1\text{MLCT}$ transitions from both $d\pi(\text{Ir}) \rightarrow \pi^*(\text{pyridylidene})$ and $d\pi(\text{Ir}) \rightarrow \pi^*(\text{ppy})$ according to time-dependent density functional theory (TDDFT) calculations (Figure S5 and Tables S4 and S5). The weak absorptions beyond 450 nm ($\epsilon < 0.8 \times 10^3 \text{ M}^{-1} \text{ cm}^{-1}$) for **1** and beyond 420 nm ($\epsilon < 2.3 \times 10^3 \text{ M}^{-1} \text{ cm}^{-1}$) for **5** are assigned as a combination of $^1\text{MLCT}$ and $^3\text{MLCT}$ transitions from $d\pi(\text{Ir}) \rightarrow \pi^*(\text{pyridylidene})$.

Complexes **1**–**8** display broad featureless emission spectra in deaerated CH_2Cl_2 at room temperature (Figures 2 and S6). The emission maxima range from 516 to 682 nm with lifetimes of up

to 3.0 μs and quantum yields of up to 0.81 (Table 1). Alcoholic glass (77 K) and solid (298 and 77 K) emission spectra were also measured (Table S3 and Figures S7–S9). Complexes **1**–**8** display markedly blue-shifted emission at 77 K glass and, in particular, a vibronic spectral feature was observed for **2**–**8** with spacing of ca. 1200–1500 cm^{-1} (Figures 2 and S7). A more detailed photophysical study on **5**, as a representative for **2**–**8**, was performed to elucidate these spectral changes. The 298 K fluid emission of **5** is slightly sensitive to the polarity of the solvents ($\Delta\lambda_{\text{max}} < 7$ nm; Figure S10), yet the large radiative rate constant, on the order of 10^5 s^{-1} , is in favor of a predominate $^3\text{MLCT}$ excited state.¹³ Besides, considerable $^3\text{MLCT}$ character is presumably preserved for 77 K glass emission, despite the distinct vibronic emission profile, because the emission lifetime ($\tau = 5.0 \mu\text{s}$) and quantum yield ($\phi = 0.94$) are comparable to those in fluid at 298 K. Variable-temperature emission measurements on **5** in an alcoholic mixture revealed a significant spectral change at ca. -130 °C, the temperature at which a liquid-to-glass transition of the alcoholic mixture takes place (Figure S11). This finding indicates that the change in the emission from 298 to 77 K is a rigidochromic effect in which the rigid medium at 77 K hinders the solvent molecules from stabilizing the charge-transfer excited state and results in a hypochromic shift in the emission. A similar luminescence rigidochromism was reported for other cationic iridium complexes.^{4b,14} The transient absorption difference spectrum of **5** is different from that of *fac*-Ir(ppy)₃, suggesting that the excited state of **5** is not associated with ppy (Figure S13). Furthermore, complexes [Ir(ppz)₂(4-R-iso-BIPY)]PF₆ (R = ^tBu for **9** and NMe₂ for **10**) emit at 586 and 516 nm (Table 1) respectively, which is equalvent to 286.3 and 222.8 cm^{-1} energy reduction with respect to the ppy analogues **1** and **5** (Figure S12). The marginal energy difference in emission upon switching the cyclometalated ligand from ppy to ppz indicates the emissive excited state of [Ir(C^N)₂(4-R-iso-BIPY)]PF₆ complexes in this work to be $^3\text{MLCT}$ associated with pyridylidene rather than with cyclometalated ligands.^{4a} This assignment is in line with spin-density calculations of the T₁ state of **1a** (model compound of **1**) and **5** in which the spin density is mainly contributed from the iridium (0.65 for **1a** and 0.65 for **5**) and pyridylidene (1 for **1a** and 1.04 for **5**) with a minor contribution from ppy (2ppy; 0.35 for **1a** and 0.31 for **5**; Figure S14).

The cyclic voltammogram of **1**–**10** features an irreversible/quasi-reversible oxidation peak (except **8**, with an additional oxidation peak) with E_{pa} from +0.51 to +0.97 V (vs Fc^{+/0}) and an irreversible reduction peak with E_{pc} from -2.16 to -1.56 V (vs Fc^{+/0}) (Table S6 and Figure S15). The E_{pa} values are +0.97 and +0.82 V, while the E_{pc} values are -1.75 and -2.13 V for **1** and **5**, respectively. It is evident that the amino substituent on pyridinium-derived NHC destabilizes both highest occupied molecular orbital (HOMO) and lowest unoccupied molecular orbital (LUMO) but to a larger extent in LUMO. As inferred from DFT calculations, where HOMO and LUMO are mainly localized on the Ir^{III} ion and pyridylidene, respectively (Figure S14), the oxidation is assigned to Ir^{III} to Ir^{IV} with some contribution from ppy, while the reduction occurs at the pyridylidene. The excited-state redox potentials $E(\text{Ir}^{\text{IV/III}*})$ and $E(\text{Ir}^{\text{III}*/\text{II}})$ are estimated based on the E_{0-0} and electrochemical data (Table S6). When the R group of the pyridylidene ligand was changed, powerful one-electron photoreductant **5** with $E(\text{Ir}^{\text{IV/III}*}) = -1.87$ V vs Fc^{+/0} and photooxidant **1** with $E(\text{Ir}^{\text{III}*/\text{II}}) = +0.71$ V vs Fc^{+/0}, which is more oxidizing than

$[\text{Ru}(\text{bpm})_3]^{2+}$ [bpm = 2,2'-bipyrimidine; $E(\text{Ru}^{\text{II}*}/\text{I}) = +0.61 \text{ V vs Fc}^{+/0}$], could be obtained.¹⁵

Visible-light-driven thiol–ene reaction was chosen to demonstrate the oxidizing nature of the excited state of **1**.¹⁶ In the presence of 0.3 mol % **1** and 0.5 equiv of *p*-toluidine as the radical mediator, the reaction of benzylmercaptan with cyclohexene under blue LED irradiation for 1 h affords the corresponding thiol–ene coupling product in 88% yield (entry 1, Tables 2 and S7). The reaction is also compatible with

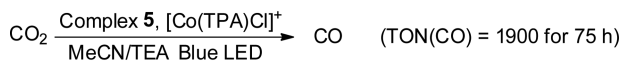
Table 2. Visible-Light-Catalyzed Radical Thiol–Ene Additions Using **1 as a Photocatalyst^a**

$\text{Ph-CH}_2\text{-SH} + \text{R} \xrightarrow[\text{Blue LED, MeCN, air, rt, 1-2 h}]{\text{Complex 1 (0.3 mol\%)}, \text{p-toluidine (0.5 equiv)}} \text{Ph-CH}_2\text{-S-CH}_2\text{-R}$			
entry (1)		(2)	(3)
	88% (55 ^c ; 82 ^d ; 81% ^e)	81% (70% ^c)	79% (Z/E = 2.6:1) (80% (Z/E = 2.1:1) ^f)
entry (4)		(5)	(6)
	81% (68% ^c)	79% (31% ^c)	54% (31% ^c)

^aRefer to the Supporting Information for details. ^b0.1 mol % photocatalyst. ^c $[\text{Ru}(\text{bpz})_3]^{2+}$ as the photocatalyst. ^d $[\text{Ir}-(\text{dF-CF}_3\text{-ppy})_2(\text{dtbpy})]^+$ as the photocatalyst. ^e $[\text{Ir}(\text{ppy})_2(\text{dtbpy})]^+$ as the photocatalyst.

internal/terminal alkene possessing other functionalities as well as phenylacetylene that furnishes the respective thiol–ene products in 54–81% yields (entries 2–6, Tables 2 and S7). Indeed, these results were generally better than those obtained from $[\text{Ru}(\text{bpz})_3]^{2+}$ [$E(\text{Ru}^{\text{II}*}/\text{I}) = +1.07 \text{ V vs Fc}^{+/0}$;^{15b} entries 1–6, Table 2] and comparable to those of $[\text{Ir}-(\text{dF-CF}_3\text{-ppy})_2(\text{dtbpy})]^+$ and $[\text{Ir}(\text{ppy})_2(\text{dtbpy})]^+$ [$\text{dF-CF}_3\text{-ppy} = 2-(2,4\text{-difluorophenyl})-5-(\text{trifluoromethyl})\text{pyridine anion}$ and $\text{dtbpy} = 4,4'\text{-di-tert-butyl-2,2'-bipyridine}$; $E(\text{Ir}^{\text{III}*}/\text{II}) = +0.83$ and $+0.28 \text{ V}$, respectively, vs $\text{Fc}^{+/0}$;^{15b} entry 1, Table 2]. The highly reducing nature of the excited state (vide supra) and the one-electron-reduced form [$E(\text{Ir}^{\text{III}}/\text{II}) = -2.13 \text{ V vs Fc}^{+/0}$] empowers **5** to mediate a visible-light-driven CO_2 reduction. Under blue LED irradiation, the reduction of CO_2 using a **5** + $[\text{Co}(\text{TPA})\text{Cl}]\text{Cl}$ protocol achieves TON(CO) up to 1900 in 75 h (Scheme 2).

Scheme 2. Visible-Light-Driven CO_2 Reduction to CO Using a **5 (0.4 mM) + $[\text{Co}(\text{TPA})\text{Cl}]\text{Cl}$ (5 μM) Protocol**



This protocol offers the following merits over the reported [*fac*- $\text{Ir}(\text{ppy})_3$ + $[\text{Co}(\text{TPA})\text{Cl}]\text{Cl}$] protocol:¹⁷ (i) higher TON(CO) (i.e., 1900 vs 1500); (ii) higher efficiency upon solar-to-fuel conversion (i.e., $\text{CO} + \text{H}_2 = 86$ vs 33 μmol); (iii) a high CO production rate is maintained even after 10 h of irradiation (Figure S16).

Unlike **2**–**6**, the amino substituent of **7** and **8** is intervened by an aryl group and not directly attached to the pyridylidene ring. Such structural feature reduces the degree of delocalization of π electron of the amino substituent toward the pyridylidene ring, which, in turn, enhances the availability of π electron against the local environment. Thus, it is envisioned that **7** and **8** could potentially be applied for pH sensing. As a proof-of-concept, when an acetonitrile solution of **8** (20 μM) was treated with

tosylic acid of increasing concentration (0–120 μM), it was observed that the low-energy absorption band collapsed gradually, while the emission intensity was attenuated by ca. 50% (Figure 4).

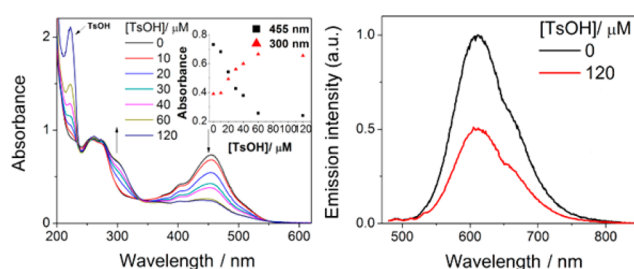


Figure 4. Left: UV–vis spectral change of **8** (20 μM) in a 0.05 M $[\text{Bu}_4\text{N}]\text{PF}_6\text{-MeCN}$ solution containing various $[\text{TsOH}]$ (0–120 μM). Inset: Plot of the absorbance at 455 and 300 nm against $[\text{TsOH}]$. Right: Emission spectra of **8** (20 μM) in a 0.05 M $[\text{Bu}_4\text{N}]\text{PF}_6\text{-MeCN}$ solution in the presence of 0 and 120 μM TsOH.

In summary, a series of luminescent iridium complexes supported by pyridinium-derived NHC ligands were synthesized. Their electronic and photophysical properties can be modified via a simple modification of pyridinium-derived NHC ligands. These iridium complexes are versatile photocatalysts and can be used in both photooxidation and -reduction reactions. We also demonstrated that this class of complexes could have potential application in pH sensing.

■ ASSOCIATED CONTENT

Supporting Information

The Supporting Information is available free of charge on the ACS Publications website at DOI: 10.1021/acs.inorgchem.7b00955.

Experimental procedures, computational details, Tables S1–S11, Figures S1–S20, Scheme S1, X-ray crystal structures of **1**, **2**, **5**, and **10** (PDF)

Accession Codes

CCDC 1546477–1546479 and 1546489 contain the supplementary crystallographic data for this paper. These data can be obtained free of charge via www.ccdc.cam.ac.uk/data_request/cif, or by emailing data_request@ccdc.cam.ac.uk, or by contacting The Cambridge Crystallographic Data Centre, 12 Union Road, Cambridge CB2 1EZ, UK; fax: +44 1223 336033.

■ AUTHOR INFORMATION

Corresponding Author

*E-mail: joeltl@hku.hk.

ORCID

Tsz Lung Lam: 0000-0002-6610-9338

Rajasekar Reddy Annapureddy: 0000-0001-5855-4688

Sharon Lai-Fung Chan: 0000-0003-0274-7258

Notes

The authors declare no competing financial interest.

[§]Deceased July 16, 2017.

■ ACKNOWLEDGMENTS

This work is supported by The Hong Kong Polytechnic University, the Hong Kong Research Grants Council (UGC; PolyU 253038/15P; AoE/P-03/08) and RGC's support for German Academic Exchange Service.

REFERENCES

- (1) Owen, J. S.; Labinger, J. A.; Bercaw, J. E. Pyridinium-Derived N-Heterocyclic Carbene Complexes of Platinum: Synthesis, Structure and Ligand Substitution Kinetics. *J. Am. Chem. Soc.* **2004**, *126*, 8247–8255.
- (2) (a) Piro, N. A.; Owen, J. S.; Bercaw, J. E. Pyridinium-derived N-heterocyclic Carbene Ligands: Syntheses, Structures and Reactivity of N-(2'-pyridyl)pyridin-2-ylidene Complexes of Nickel(II), Palladium(II) and Platinum(II). *Polyhedron* **2004**, *23*, 2797–2804. (b) Ionkin, A. S.; Marshall, W. J.; Roe, D. C.; Wang, Y. Synthesis, Structural Characterization and the First Electroluminescent Properties of Tris- and Bis-Cycloiridiated Complexes of Sterically Hindered Electron-Poor 2-(3,5-bis(trifluoromethyl)phenyl)-4-trifluoromethylpyridine. *Dalton Trans.* **2006**, 2468–2478. (c) Moussa, J.; Freeman, G. R.; Williams, J. A. G.; Chamoreau, L.-M.; Herson, P.; Amouri, H. Synthesis and Luminescence Properties of Cycloplatinated Complexes with a Chelating N⁴C Pyridine-Derived N-Heterocyclic Carbene – Influence of 2,4,6-Triphenylphosphinine versus Triphenylphosphine. *Eur. J. Inorg. Chem.* **2016**, *2016*, 761–767. (d) Tseng, C.-H.; Fox, M. A.; Liao, J.-L.; Ku, C.-H.; Sie, Z.-T.; Chang, C.-H.; Wang, J.-Y.; Chen, Z.-N.; Lee, G.-H.; Chi, Y. Luminescent Pt(II) Complexes Featuring Imidazolylidene-pyridylidene and Dianionic Bipyrazolate: from Fundamentals to OLED Fabrications. *J. Mater. Chem. C* **2017**, *5*, 1420–1435.
- (3) (a) Koizumi, T.-a.; Tomon, T.; Tanaka, K. Synthesis and Electrochemical Properties of Bis(bipyridine)ruthenium(II) Complexes Bearing Pyridinyl- and Pyridinylidene Ligands Induced by Cyclometalation of N'-Methylated Bipyridinium Analogs. *J. Organomet. Chem.* **2005**, *690*, 1258–1264. (b) Song, G.; Zhang, Y.; Su, Y.; Deng, W.; Han, K.; Li, X. Pyridine-Based N-Heterocyclic Carbene Hydride Complexes of Iridium via C–H Activation. *Organometallics* **2008**, *27*, 6193–6201. (c) Schuster, O.; Yang, L.; Raubenheimer, H. G.; Albrecht, M. Beyond Conventional N-Heterocyclic Carbenes: Abnormal, Remote, and Other Classes of NHC Ligands with Reduced Heteroatom Stabilization. *Chem. Rev.* **2009**, *109*, 3445–3478. (d) Guisado-Barrios, G.; Bouffard, J.; Donnadiu, B.; Bertrand, G. Bis(1,2,3-triazol-5-ylidenes) (i-bitz) as Stable 1,4-Bidentate Ligands Based on Mesoionic Carbenes (MICs). *Organometallics* **2011**, *30*, 6017–6021. (e) Yoshidomi, T.; Segawa, Y.; Itami, K. Pyridine-Based Dicarbene Ligand: Synthesis and Structure of a Bis-2-pyridylidene Palladium Complex. *Chem. Commun.* **2013**, *49*, 5648–5650. (f) Coe, B. J.; Helliwell, M.; Sánchez, S.; Peers, M. K.; Scrutton, N. S. Water-soluble Ir(III) Complexes of Deprotonated N-Methylbipyridinium Ligands: Fluorine-Free Blue Emitters. *Dalton Trans.* **2015**, *44*, 15420–15423. (g) Coe, B. J.; Helliwell, M.; Raftery, J.; Sánchez, S.; Peers, M. K.; Scrutton, N. S. Cyclometalated Ir(III) Complexes of Deprotonated N-Methylbipyridinium Ligands: Effects of Quaternised N Centre Position on Luminescence. *Dalton Trans.* **2015**, *44*, 20392–20405.
- (4) (a) Lowry, M. S.; Goldsmith, J. I.; Slinker, J. D.; Rohl, R.; Pascal, R. A., Jr.; Malliaras, G. G.; Bernhard, S. Single-Layer Electroluminescent Devices and Photoinduced Hydrogen Production from an Ionic Iridium(III) Complex. *Chem. Mater.* **2005**, *17*, 5712–5719. (b) Tamayo, A. B.; Garon, S.; Sajoto, T.; Djurovich, P. I.; Tsyba, I. M.; Bau, R.; Thompson, M. E. Cationic Bis-cyclometalated Iridium(III) Diimine Complexes and Their Use in Efficient Blue, Green, and Red Electroluminescent Devices. *Inorg. Chem.* **2005**, *44*, 8723–8732. (c) Nazeeruddin, M. K.; Wegh, R. T.; Zhou, Z.; Klein, C.; Wang, Q.; De Angelis, F.; Fantacci, S.; Grätzel, M. *Inorg. Chem.* **2006**, *45*, 9245–9250. (d) Su, H.-C.; Chen, H.-F.; Fang, F.-C.; Liu, C.-C.; Wu, C.-C.; Wong, K.-T.; Liu, Y.-H.; Peng, S.-M. Solid-State White Light-Emitting Electrochemical Cells Using Iridium-Based Cationic Transition Metal Complexes. *J. Am. Chem. Soc.* **2008**, *130*, 3413–3419. (e) Costa, R. D.; Orta, E.; Bolink, H. J.; Graber, S.; Schaffner, S.; Neuburger, M.; Housecroft, C. E.; Constable, E. C. Archetype Cationic Iridium Complexes and Their Use in Solid-State Light-Emitting Electrochemical Cells. *Adv. Funct. Mater.* **2009**, *19*, 3456–3463. (f) Ulbricht, C.; Beyer, B.; Friebe, C.; Winter, A.; Schubert, U. S. Recent Developments in the Application of Phosphorescent Iridium(III) Complex Systems. *Adv. Mater.* **2009**, *21*, 4418–4441. (g) Hu, T.; He, L.; Duan, L.; Qiu, Y. Solid-state light-emitting electrochemical cells based on ionic iridium(III) complexes. *J. Mater. Chem.* **2012**, *22*, 4206–4215. (h) Henwood, A. F.; Zysman-Colman, E. Lessons learned in tuning the optoelectronic properties of phosphorescent iridium(III) complexes. *Chem. Commun.* **2017**, *53*, 807–826.
- (5) Goldsmith, J. I.; Hudson, W. R.; Lowry, M. S.; Anderson, T. H.; Bernhard, S. Discovery and High-Throughput Screening of Heteroleptic Iridium Complexes for Photoinduced Hydrogen Production. *J. Am. Chem. Soc.* **2005**, *127*, 7502–7510.
- (6) (a) Zhao, Q.; Li, F.; Liu, S.; Yu, M.; Liu, Z.; Yi, T.; Huang, C. Highly Selective Phosphorescent Chemosensor for Fluoride Based on an Iridium(III) Complex Containing Arylborane Units. *Inorg. Chem.* **2008**, *47*, 9256–9264. (b) Lo, K. K.-W.; Li, S. P.-Y.; Zhang, K. Y. Development of luminescent iridium(III) polypyridine complexes as chemical and biological probes. *New J. Chem.* **2011**, *35*, 265–287. (c) Guerschais, V.; Fillaut, J.-L. Sensory luminescent iridium(III) and platinum(II) complexes for cation recognition. *Coord. Chem. Rev.* **2011**, *255*, 2448–2457. (d) Ma, D.-L.; Lin, S.; Wang, W.; Yang, C.; Leung, C.-H. Luminescent chemosensors by using cyclometalated iridium(III) complexes and their applications. *Chem. Sci.* **2017**, *8*, 878–889.
- (7) You, Y. Phosphorescence bioimaging using cyclometalated Ir(III) complexes. *Curr. Opin. Chem. Biol.* **2013**, *17*, 699–707.
- (8) (a) Nagib, D. A.; Scott, M. E.; MacMillan, D. W. C. Enantioselective α -Trifluoromethylation of Aldehydes via Photoredox Organocatalysis. *J. Am. Chem. Soc.* **2009**, *131*, 10875–10877. (b) Condie, A. G.; González-Gómez, J. C.; Stephenson, C. R. J. Visible-Light Photoredox Catalysis: Aza-Henry Reactions via C–H Functionalization. *J. Am. Chem. Soc.* **2010**, *132*, 1464–1465. (c) Tellis, J. C.; Primer, D. N.; Molander, G. A. Single-electron transmetalation in organoboron cross-coupling by photoredox/nickel dual catalysis. *Science* **2014**, *345*, 433–436. (d) Koike, T.; Akita, M. Visible-light radical reaction designed by Ru- and Ir-based photoredox catalysis. *Inorg. Chem. Front.* **2014**, *1*, 562–576.
- (9) (a) Yang, C.-H.; Beltran, J.; Lemaur, V.; Cornil, J.; Hartmann, D.; Sarfert, W.; Fröhlich, R.; Bizzarri, C.; De Cola, L. Iridium Metal Complexes Containing N-heterocyclic Carbene Ligands for Blue-Light-Emitting Electrochemical Cells. *Inorg. Chem.* **2010**, *49*, 9891–9901. (b) Meier, S. B.; Sarfert, W.; Junquera-Hernandez, J. M.; Delgado, M.; Tordera, D.; Orti, E.; Bolink, H. J.; Kessler, F.; Scopelliti, R.; Grätzel, M.; Nazeeruddin, M. K.; Baranoff, E. A deep-blue emitting charged bis-cyclometalated iridium(III) complex for light-emitting electrochemical cells. *J. Mater. Chem. C* **2013**, *1*, 58–68. (c) Zhang, F.; Ma, D.; Duan, L.; Qiao, J.; Dong, G.; Wang, L.; Qiu, Y. Synthesis, Characterization, and Photophysical and Electroluminescent Properties of Blue-Emitting Cationic Iridium(III) Complexes Bearing Nonconjugated Ligands. *Inorg. Chem.* **2014**, *53*, 6596–6606.
- (10) Yang, C.; Mehmood, F.; Lam, T. L.; Chan, S. L.-F.; Wu, Y.; Yeung, C.-S.; Guan, X.; Li, K.; Chung, C. Y.-S.; Zhou, C.-Y.; Zou, T.; Che, C.-M. Stable Luminescent Iridium(III) Complexes with Bis(N-Heterocyclic Carbene) Ligands: Photo-Stability, Excited State Properties, Visible-Light-Driven Radical Cyclization and CO₂ Reduction, and Cellular Imaging. *Chem. Sci.* **2016**, *7*, 3123–3136.
- (11) (a) Zhou, Y.; Jia, J.; Li, W.; Fei, H.; Zhou, M. Luminescent biscarbene iridium(III) complexes as living cell imaging reagents. *Chem. Commun.* **2013**, *49*, 3230–3232. (b) Li, Y.; Liu, B.; Lu, X.-R.; Li, M.-F.; Ji, L.-N.; Mao, Z.-W. Cyclometalated iridium(III) N-heterocyclic carbene complexes as potential mitochondrial anticancer and photodynamic agents. *Dalton Trans.* **2017**, DOI: 10.1039/C7DT01903C.
- (12) (a) Stringer, B. D.; Quan, L. M.; Barnard, P. J.; Wilson, D. J. D.; Hogan, C. F. Iridium Complexes of N-Heterocyclic Carbene Ligands: Investigation into the Energetic Requirements for Efficient Electro-generated Chemiluminescence. *Organometallics* **2014**, *33*, 4860–4872. (b) Monti, F.; La Placa, M. G. I.; Armaroli, N.; Scopelliti, R.; Grätzel, M.; Nazeeruddin, M. K.; Kessler, F. Cationic Iridium(III) Complexes with Two Carbene-Based Cyclometalating Ligands: Cis Versus Trans Isomers. *Inorg. Chem.* **2015**, *54*, 3031–3042.
- (13) Sajoto, T.; Djurovich, P. I.; Tamayo, A. B.; Osgaard, J.; Goddard, W. A., III; Thompson, M. E. Temperature Dependence of Blue Phosphorescent Cyclometalated Ir(III) Complexes. *J. Am. Chem. Soc.* **2009**, *131*, 9813–9822.

(14) Ladouceur, S.; Zysman-Colman, E. A Comprehensive Survey of Cationic Iridium(III) Complexes bearing Nontraditional Ligand Chelation Motifs. *Eur. J. Inorg. Chem.* **2013**, *2013*, 2985–3007.

(15) The excited-state reduction potential of $[\text{Ru}(\text{bpm})_3]^{2+}$ versus saturated calomel electrode was obtained from the following references:

(a) Rillema, D. P.; Allen, G.; Meyer, T. J.; Conrad, D. Redox Properties of Ruthenium(II) Tris Chelate Complexes Containing the Ligands 2,2'-bipyrazine, 2,2'-bipyridine, and 2,2'-bipyrimidine. *Inorg. Chem.* **1983**, *22*, 1617–1622. (b) Prier, C. K.; Rankic, D. A.; MacMillan, D. W. C. Visible Light Photoredox Catalysis with Transition Metal Complexes: Applications in Organic Synthesis. *Chem. Rev.* **2013**, *113*, 5322–5363.

Its excited state reduction potential against the ferrocenium/ferrocene ($\text{Fc}^{+/0}$) couple was calculated according to the following references: (c) Connelly, N. G.; Geiger, W. E. Chemical Redox Agents for Organometallic Chemistry. *Chem. Rev.* **1996**, *96*, 877–910. (d) Pavlishchuk, V. V.; Addison, A. W. Conversion constants for redox potentials measured versus different reference electrodes in acetonitrile solutions at 25 °C. *Inorg. Chim. Acta* **2000**, *298*, 97–102.

(16) Tyson, E. L.; Niemeyer, Z. L.; Yoon, T. P. Redox Mediators in Visible Light Photocatalysis: Photocatalytic Radical Thiol–Ene Additions. *J. Org. Chem.* **2014**, *79*, 1427–1436.

(17) Chan, S. L.-F.; Lam, T. L.; Yang, C.; Yan, S.-C.; Cheng, N. M. A Robust and Efficient Cobalt Molecular Catalyst for CO_2 Reduction. *Chem. Commun.* **2015**, *51*, 7799–7801.